

1 **A practical guideline of genomics-driven drug discovery in the era of** 2 **global biobank meta-analysis**

3

4 Shinichi Namba^{1,10}, Takahiro Konuma^{1,2,10}, Kuan-Han Wu³, Wei Zhou^{4,5}, Global Biobank
5 Meta-analysis Initiative, and Yukinori Okada^{1,6-9,11}

6

7 ¹Department of Statistical Genetics, Osaka University Graduate School of Medicine, Suita
8 565-0871, Japan.

9 ²Central Pharmaceutical Research Institute, JAPAN TOBACCO INC., Takatsuki 569-1125,
10 Japan.

11 ³Department of Computational Medicine and Bioinformatics, University of Michigan, Ann
12 Arbor, MI, USA.

13 ⁴Analytic and Translational Genetics Unit, Department of Medicine, Massachusetts General
14 Hospital, Boston, Massachusetts, USA.

15 ⁵Stanley Center for Psychiatric Research, Broad Institute of MIT and Harvard, Cambridge,
16 Massachusetts, USA.

17 ⁶Laboratory for Systems Genetics, RIKEN Center for Integrative Medical Sciences,
18 Yokohama 230-0045, Japan.

19 ⁷Laboratory of Statistical Immunology, Immunology Frontier Research Center (WPI-IFReC),
20 Osaka University, Suita 565-0871, Japan.

21 ⁸Integrated Frontier Research for Medical Science Division, Institute for Open and
22 Transdisciplinary Research Initiatives, Osaka University, Suita 565-0871, Japan.

23 ⁹Center for Infectious Disease Education and Research (CiDER), Osaka University, Suita
24 565-0871, Japan.

25 ¹⁰NOTE: This preprint reports new research that has not been certified by peer review and should not be used to guide clinical practice.
¹⁰These authors contributed equally.

26 ¹¹Corresponding author, Yukinori Okada (yokada@sg.med.osaka-u.ac.jp)

27

28 Yukinori Okada, M.D., Ph.D.

29 Address: 2-2 Yamadaoka, Suita, Osaka 565-0871, Japan

30 Phone: +81-6-6879-3971

31 E-mail: yokada@sg.med.osaka-u.ac.jp

32 **Summary**

33 Genomics-driven drug discovery is indispensable for accelerating the development of novel
34 therapeutic targets. However, the drug discovery framework based on evidence from
35 genome-wide association studies (GWAS) has not been established, especially for cross-
36 population GWAS meta-analysis. Here, we introduce a practical guideline for genomics-
37 driven drug discovery for cross-population meta-analysis, as lessons from the Global Biobank
38 Meta-analysis Initiative (GBMI). Our drug discovery framework encompassed three
39 methodologies and was applied to the 13 common diseases targeted by GBMI ($N_{\text{mean}} =$
40 1,329,242). First, we evaluated the overlap enrichment between disease risk genes and the
41 drug-target genes of the disease-relevant medication categories. An omnibus approach
42 integrating the four gene prioritization tools yielded twice the enrichment in the disease-
43 relevant medication categories compared with any single tool, and identified drugs with
44 approved indications for asthma, gout, and venous thromboembolism. Second, we performed
45 an endophenotype Mendelian randomization analysis using protein quantitative trait loci as
46 instrumental variables. After the application of quality controls, including a colocalization
47 analysis, significant causal relationships were estimated for 18 protein–disease pairs,
48 including MAP2K inhibitors for heart failure. Third, we conducted an *in silico* screening for
49 negative correlations between genetically determined disease case–control gene expression
50 profiles and compound-regulated ones. Significant negative correlations were observed for
51 31 compound–disease pairs, including a histone deacetylase inhibitor for asthma. Integration
52 of the three methodologies provided a comprehensive catalog of candidate drugs for
53 repositioning, nominating promising drug candidates targeting the genes involved in the
54 coagulation process for venous thromboembolism. Our study highlighted key factors for
55 successful genomics-driven drug discovery using cross-population meta-analysis.

56

57 **Keywords**

58 Genomics-driven drug discovery, genome-wide association study, cross-population meta-
59 analysis, gene prioritization, Mendelian randomization, genetically regulated gene expression

60 Introduction

61 Efficient screening of novel therapeutic targets is an essential process to accelerate drug
62 discovery. Despite the enormous effort to develop novel drugs, the overall success rate of
63 clinical application has been decreasing because of the considerable increase in both the
64 cost and the duration¹. Genomics-driven drug discovery is one of the promising solutions, as
65 drug targets with human genetic support are more likely to be successful in clinical
66 development^{2,3}. In particular, rare-variant studies for mendelian diseases have led to drug
67 development, such as *PSCK9* inhibitors for low-density lipoprotein cholesterol⁴. For common
68 diseases, genome-wide association studies (GWAS) have provided valuable opportunities
69 for drug discovery; nevertheless, drug discovery based on GWAS remains challenging⁵. Few
70 bioinformatics tools directly prioritize candidate drugs⁶, and there exist no practical guidelines
71 regarding how to conduct genomics-driven drug discovery.

72 Recently, an increasing number of large-scale GWAS meta-analyses of multiple
73 populations have been carried out. These have revealed key insights into the biological
74 processes underlying complex diseases^{7,8}, thus affording the possibility of in-depth
75 application of genomics-driven drug discovery. However, the majority of previous genomics-
76 driven drug discovery projects were carried out for GWAS of a single ancestry of Europeans⁶,
77 and there are few successful applications to cross-population GWAS meta-analyses. The
78 global heterogeneity in genetic background (e.g., different allele frequencies and linkage
79 disequilibrium [LD]) among populations makes it difficult to perform downstream analyses
80 such as gene expression prediction⁹ and colocalization analysis¹⁰. In addition, causal effect
81 sizes are population-specific especially in functionally important regions¹¹. Therefore, a
82 specialized drug discovery framework is required for cross-population GWAS meta-analyses.

83 In this study, we introduce a practical guideline as lessons from the Global Biobank
84 Meta-analysis Initiative (GBMI)⁷. GBMI meta-analyzed GWASs of global biobanks from
85 diverse ancestries incorporating several recruitment strategies (e.g., population-based or

86 hospital-based biobanks), including up to 1.8 million participants from the 18 biobanks in four
87 continents (341,000 East Asians (EAS); 31,000 Central and South Asians; 33,000 Africans;
88 18,000 Admixed Americans; 1,600 Middle Easterners; 156,000 Finns; and 1,220,000 Non-
89 Finnish Europeans [NFE]), serving as a gold-standard cross-population GWAS meta-analysis.

90 We propose a cross-population drug discovery framework comprising three major
91 methodologies. First, overlap enrichment of disease risk genes with targets of existing
92 drugs^{12–14} identifies drug repurposing opportunities. Second, endophenotype Mendelian
93 randomization (MR), and subsequent quality controls, including colocalization analyses¹⁵
94 establishes causal links between proteins and disease processes. Lastly, screening of
95 negative correlations between genetically regulated disease case–control gene expression
96 (GReX) and compound-regulated gene expression profiles¹⁶ can be used to identify
97 compounds that might correct disease-related alterations in gene expression.

98 We applied our framework to the 13 common and relatively rare disease GWAS included
99 in GBMI: asthma, primary open-angle glaucoma (POAG), gout, chronic obstructive
100 pulmonary disease (COPD), venous thromboembolism (VTE), thyroid cancer (ThC),
101 abdominal aortic aneurysm (AAA), heart failure (HF), idiopathic pulmonary fibrosis (IPF),
102 stroke, uterine cancer (UtC), acute appendicitis (AcApp), and hypertrophic cardiomyopathy
103 (HCM). Our pipeline identified 144 drug/compound-disease pairs and nominated a
104 comprehensive catalog of candidate drugs for repositioning. Our study demonstrates that the
105 integration of the candidate drugs and compounds screened using each methodology
106 enables in-depth drug discovery. In particular, drug discovery captured plausible drug targets
107 targeting coagulation-related genes for VTE. Our results demonstrated the utility of
108 genomics-driven drug discovery using a cross-population GWAS meta-analysis and suggest
109 key factors for successful drug discovery.

110

111 Results

112 Overview of the genomics-driven drug discovery framework

113 Various types of omics-based approaches have been proposed for novel target identification
114 and drug repositioning from GWAS summary statistics⁶. Each type of omics data necessitates
115 specialized methodologies. Further, no simple method has emerged that enables the
116 interpretation of genomics-discoveries for drug discovery. Therefore, our framework was
117 composed of three parts, in which each component utilized different external omics data and
118 knowledge bases to obtain biological insights from GWAS summary statistics (**Figure 1**), as
119 follows. (i) First, we performed an overlap enrichment analysis of the disease risk genes with
120 the target genes of existing drugs^{12–14}. Gene prioritization tools summarized variant-level *P*-
121 values at the gene level, and the pharmacological agents targeting the prioritized genes
122 served as drug candidates. Genes that are modulated by approved drugs are known to be
123 enriched in disease-relevant clinical classifications, such as drug medication categories (i.e.,
124 Anatomical Therapeutic Chemical Classification System [ATC]) and disease categories (i.e.,
125 International Statistical Classification of Diseases and Related Health Problems [ICD-10])^{13,14},
126 which were utilized to assess the validity of the drug candidates. (ii) Second, we performed
127 endophenotype MR and subsequent quality controls, including colocalization analyses¹⁵. MR
128 is a method that is used for estimating the causal effect of one trait (exposure) on another
129 trait (outcome) using genetic variants as instrument variables (IVs)¹⁷. We used the lead
130 variants of the protein quantitative trait loci (pQTL) as IVs to examine the disease-causing
131 effects of the proteins. Subsequent quality controls were effective in avoiding false-positive
132 causalities¹⁸. Particularly, colocalization analysis is an important step for the exclusion of
133 confounding by LD. (iii) Finally, we performed a screening of negative correlations between
134 genetically regulated disease case–control gene expression (GReX) and compound-
135 regulated gene expression profiles¹⁶. Transcriptome-wide association studies (TWAS) use
136 expression QTL (eQTL) acting in *cis* to impute disease-specific GReX from the GWAS

137 summary statistics⁹. The compounds that have inverse effects on gene expression against
138 case–control GReX serve as candidates for the disease of interest^{16,19}. We imputed GReX
139 for the tissues included in the Genotype-Tissue Expression project (GTEx) v7²⁰ and used
140 compound-induced gene expression profiles for thousands of compounds in various
141 conditions and cell lines collected in one of the largest public databases available, the Library
142 of Integrated Network-based Cellular Signatures project (LINCS) L1000 connectivity map²¹.
143

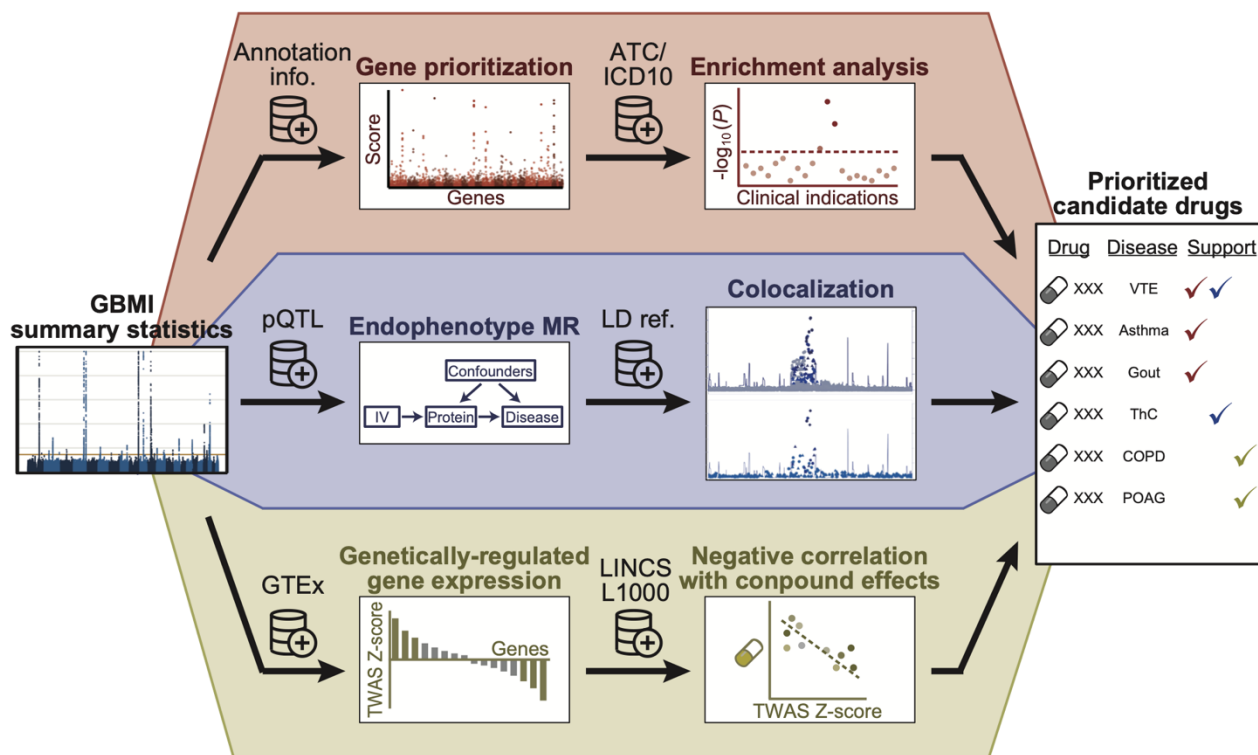


Figure 1. Overview of the genomics-driven drug discovery framework.

The framework consisted of three components. Each component utilizes the summary statistics of genome-wide association analyses and external resources to prioritize candidate drugs. GBMI, Global Biobank Meta-analysis Initiative; ATC, Anatomical Therapeutic Chemical Classification System; ICD10, International Statistical Classification of Diseases and Related Health Problems; pQTL, protein quantitative trait loci; LD, linkage disequilibrium; MR, Mendelian randomization; GTEx, the Genotype-Tissue Expression project; TWAS, transcriptome-wide association study; LINCS, the Library of Integrated Network-based Cellular Signatures project.

144

145

146

147 **Overlap enrichment of disease risk genes in medication categories**

148 The first component prioritized disease risk genes by calculating gene scores or *P*-values,
149 and examined whether the prioritized genes are enriched in drug-target genes of specific
150 medication categories. There exist several gene prioritization tools, although it remains
151 unclear which tool is best optimized for drug discovery. Therefore, we evaluated four tools in
152 parallel, i.e., MAGMA²², DEPICT²³, Priority index (Pi)⁵, and Polygenic Priority Score (PoPS)²⁴.
153 MAGMA is a simple method that is used to summarize variant-level *P*-values according to
154 gene positions and LD structure. The prioritized genes by MAGMA were nominally
155 overlapped with drug-target genes in the disease-relevant ATC codes for Gout, COPD, and
156 VTE ($P < 0.05$; **Supplementary Figure 1A**). DEPICT, which uses co-regulated gene
157 expression for gene prioritization²³, showed clearer enrichment than did MAGMA for gout and
158 VTE; however, no genes were prioritized for diseases with a relatively small number of
159 genome-wide significant loci, such as IPF and UtC (**Supplementary Figure 1B**). Pi is a
160 scoring system that was designed for drug development of immune-related diseases, and
161 integrates multiple annotations, including eQTL, chromatin interaction, and genes implicated
162 in immune functions⁵. The genes targeted by antineoplastic and immunomodulating agents
163 were enriched for all diseases using Pi (**Supplementary Figure 1C**), suggesting that Pi could
164 specifically provide enrichment of the immune genes regardless of the disease categories,
165 even including non-immune diseases. PoPS estimates responsible genes using various gene
166 features, such as cell-type-specific gene expression and biological pathways²⁴. We observed
167 enrichment of drug-target genes for broad ATC codes, suggesting that PoPS provided
168 relatively high scores for the entire drug-target gene collection, regardless of their medication
169 categories (**Supplementary Figure 1D**). We replicated the analyses using ICD-10 and
170 observed a similar pattern of enrichment as ATC codes (**Supplementary Figure 2**).

171 Next, we summarized the overlap enrichment into disease-relevant and disease-

172 irrelevant medication categories across the diseases. For both ATC and ICD-10 codes, all
173 tools confirmed enrichment in the relevant codes, although a relatively high enrichment in the
174 irrelevant codes was also observed for Pi and PoPS (**Figure 2A–C and Supplementary**
175 **Figure 3**), reflecting biased enrichment in immune genes and non-specific enrichment in
176 drug-target genes, respectively. DEPICT yielded a lower enrichment in irrelevant codes than
177 did MAGMA. As a sensitivity analysis, we sequentially changed the thresholds of the gene
178 scores and *P*-values. The pattern of the overall enrichment was robust for a wide range of
179 thresholds (**Supplementary Figure 4**). The enrichment of disease genes prioritized by
180 DEPICT in the relevant ATC codes became smaller with the stringent thresholds. DEPICT
181 calculates *P*-values for the genes in the genome-wide significant loci exclusively, by default;
182 therefore, liberal thresholds such as a false discovery rate (FDR) of 0.2 might be suitable for
183 DEPICT.

184 Given that the four tools separately prioritized genes according to the different
185 methodologies, we hypothesized that omnibus integration of the four methods could
186 efficiently improve the enrichment of disease-relevant drug-target genes. As an omnibus
187 approach, we selected 81 gene–disease pairs that were prioritized by all tools
188 (**Supplementary Table 1**), and showed a twice larger OR than did those of any single tool
189 for the relevant ATC codes (OR = 4.29, $P = 5.5 \times 10^{-5}$) (**Supplementary Figure 2A–C**).
190 Conversely, the enrichment in the irrelevant ATC codes (OR = 1.41, $P = 0.16$) was close to
191 that of the single tools, indicating an advantage of combining multiple gene prioritization
192 methods to increase statistical power while retaining controlled type 1 errors. We also
193 confirmed the efficacy of the omnibus strategy using ICD-10 (**Supplementary Figure 3**).

194 The examination of the omnibus results for each disease revealed an enrichment in the
195 relevant ATC codes for asthma, gout, and VTE (**Figure 2D**), which corresponded to 30 drugs
196 in total (**Supplementary Table 1**). For asthma and gout, all prioritized genes in the disease-
197 relevant ATC codes were targeted by the drugs with approved indication. The genes

198 prioritized for VTE were involved in the coagulation cascade, and four of them (*F2*, *F10*, *FGA*,
199 and *PROC*) were the approved drug targets for VTE. The prioritized genes for asthma were
200 also enriched in antineoplastic and immunomodulating agents. Although the drugs in this
201 category have not been indicated for asthma, their target genes involved immune genes,
202 such as *IL1R1*, suggesting that the omnibus approach correctly prioritized genes related to
203 asthma.

204

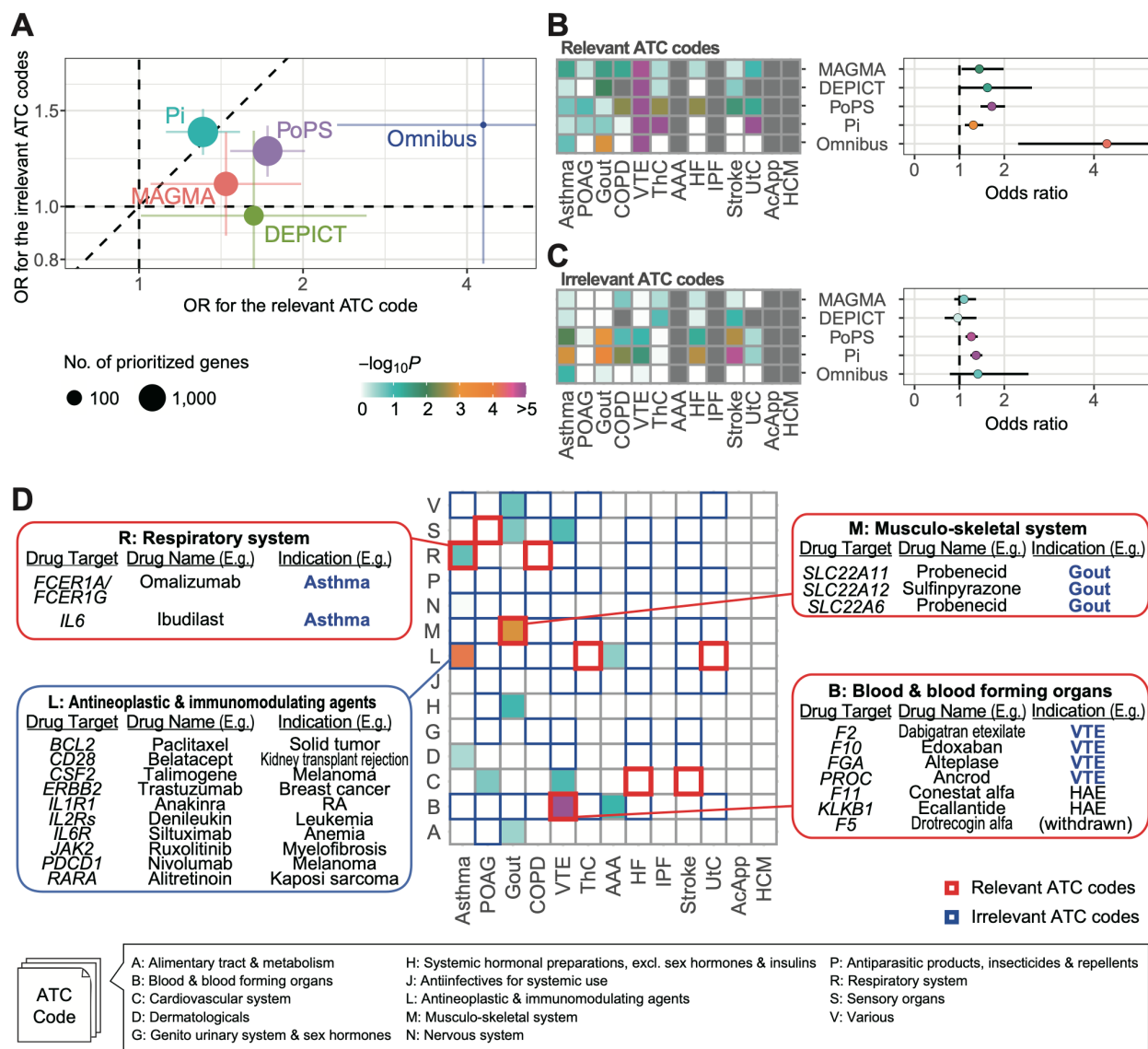


Figure 2. Enrichment of prioritized drug-target genes in the disease-relevant medication categories.

A, Overall enrichment of drug-target genes nominated by four gene prioritization tools and their omnibus results. The error bars represent 95% confidence intervals. **B** and **C**, Enrichment of the prioritized drug-target genes in the disease-relevant ATC codes (**B**) and the disease-irrelevant ATC codes (**C**). The diseases are sorted in the descending order of the number of genome-wide significant loci determined in GBMI GWAS. **D**, Enrichments for the omnibus results per disease and ATC code.

OR, odds ratio; POAG, primary open-angle glaucoma; COPD, chronic obstructive pulmonary disease; VTE, venous thromboembolism; ThC, thyroid cancer; AAA, abdominal aortic aneurysm; HF, heart failure; IPF, idiopathic pulmonary fibrosis; UtC, uterine cancer; AcApp, acute appendicitis; HCM, hypertrophic cardiomyopathy; RA, rheumatoid arthritis; HAE, acute attacks of hereditary angioedema.

206 **Endophenotype Mendelian randomization**

207 Understanding protein regulation is essential for drug discovery. Therefore, we conducted
208 MR analyses to infer disease-causing proteins^{15,25}. Although the current eQTL studies yield
209 larger sample sizes than pQTL²⁶, there exists low correlation between transcript expression
210 and protein abundance²⁷. Here, we utilized the lead variants summarized from five pQTL
211 studies^{27–31} as IVs for MR. To avoid confounding factors, such as horizontal pleiotropy, we
212 restricted IVs to those with low heterogeneity between studies and low pleiotropy between
213 proteins, whereas we used both *cis*- and *trans*-pQTL to target a wide range of proteins, as
214 described previously¹⁸ (Methods). We conducted an MR analysis using the 266 IVs
215 associated with the 229 drug-targeted proteins, to test the causal effects on the 13 diseases.
216 After applying multiple test corrections, 25 protein–disease pairs showed significant causality
217 (FDR < 0.05, **Supplementary Table 2**). Twelve pairs were derived from *cis*-pQTL, whereas
218 the remaining ones were derived from *trans*-pQTL.

219 To protect against false positives from the results of the MR analysis, we applied two
220 quality-control metrics, i.e., colocalization analysis and concordance of directional effects.
221 The colocalization analysis was used to check whether two signals were equally distributed
222 on the local LD structure. Therefore, we used the GBMI GWAS of the NFE-specific meta-
223 analysis for MR and colocalization analysis, rather than the all-ancestry meta-analysis, to
224 match the population background to the pQTL studies. All 25 pairs passed the directionality
225 check, while colocalization was confirmed for 18 pairs (**Figure 3A**). These pairs included F11
226 and PROC for VTE and PLAU for AAA, which were also prioritized by the omnibus gene
227 prioritization. In particular, F11 and PROC for VTE were also nominated by the overlap
228 enrichment analysis. The colocalization of F11–VTE is shown in **Figure 3B** as an illustrative
229 example. Most of the colocalization methods assume only a single causal variant per locus;
230 however, recent methodological advances enabled us to address the possibility of multiple
231 causal variants in one locus³². We applied coloc³³ to conditionally independent signals

232 decomposed by SuSiE³⁴. SuSiE detected three and two signals for the GWAS of VTE and
233 pQTL of F11, respectively, of which two signals were inferred to be colocalized.

234 Next, we assessed whether the inferred causal relationships were consistent with
235 clinical implications and experimental evidence. We found literature-based support of the
236 causal signs of the MR effect sizes for six protein–disease pairs (**Supplementary Table 3**).
237 For example, lipoprotein(a) (LPA) for AAA and PDGFB for VTE have been reported to be
238 disease biomarkers^{35,36}. Similarly, ApoB-containing lipoproteins were associated with
239 angiotensin II-induced AAA in a mouse model³⁷. In contrast, we found that the negative sign
240 of the MR effect size for PROC-VTE was not consistent with the knowledge that protein C,
241 which is encoded by *PROC*, itself, is used for the treatment of VTE. The pQTL of PROC was
242 identified as a *trans*-pQTL, which might confound the sign because PROC may not be the
243 direct target of the pQTL effects.

244 We curated drugs from the four major drug databases: DrugBank³⁸, Therapeutic Target
245 Database (TTD)³⁹, PharmGKB⁴⁰, and the Open Targets Platform⁴¹, resulting in 83 drugs for
246 14 protein–disease pairs (**Supplementary Table 3**). These drugs included MAP2K inhibitors
247 for HF, which experimentally ameliorate cardiac hypertrophy and cardiomyopathy^{42,43}.
248 Regarding the F11–VTE pair, an F11 inhibitor, Abelacimab, showed efficacy for the prevention
249 of VTE in a phase II trial⁴⁴. In addition, as an agonist of PLAU for asthma, the urokinase-type
250 plasminogen activator was reported to reduce airway remodeling in a mouse model⁴⁵.

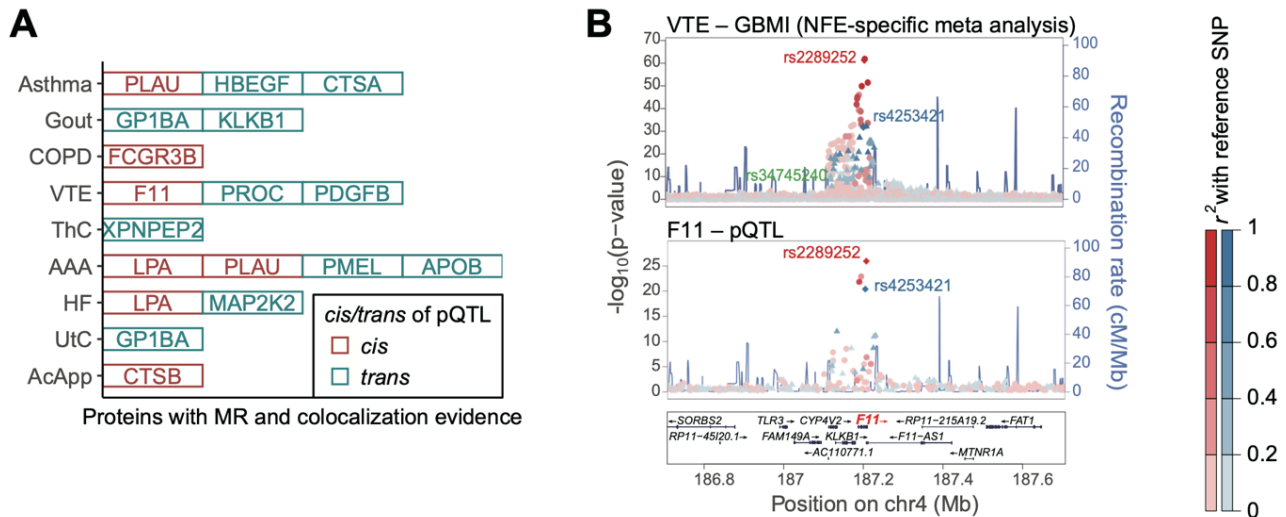


Figure 3. Endophenotype Mendelian randomization.

A, Drug-target proteins with significant causal effects inferred by Mendelian randomization and with colocalization between GBMI GWAS and protein quantitative trait loci (pQTL). **B**, LocusZoom⁶⁰ plots showing colocalization between GWAS for VTE and pQTL for F11. The fine-mapped variants are shown with their rsID.

251

252

253 **Negative correlation tests between genetically determined and compound-regulated**
254 **gene expression**

255 Finally, we performed an *in silico* screening of negative correlations between TWAS-based
256 disease case–control GReX and compound-regulated gene expression profiles¹⁶ to identify
257 compounds with a potentially beneficial effect for treatment of each disease. By matching the
258 cell and tissue specificity between TWAS (based on the GTEx tissues) and compound-
259 regulated gene expression profiles (cell lines collected in the LINCS L1000 library), we tested
260 the negative correlation for 308,872 compound–tissue–condition pairs per disease (Methods).
261 Because a large sample size and population-specific LD structure are required for robust *in*
262 *silico* estimation of GReX by TWAS⁹, we restricted our analysis to the results of the
263 population-specific meta-analyses of EAS and NFE. An EAS-specific meta-analysis was not
264 performed in GBMI for three diseases, i.e., ThC, AAA, and AcApp, which were excluded. We
265 calculated correlation coefficients in the two populations separately and subsequently
266 combined them in a random-effect meta-analysis framework. We obtained 31 compound–
267 disease pairs with an FDR < 0.05 (**Figure 4**).

268 The negative correlation tests can be applied even to compounds without known targets
269 when the compound-induced gene expression changes are assayed. In fact, most of the
270 prioritized compounds (14 out of 31) were understudied or had no known targets. These
271 compounds were valuable, because they could be therapeutic drugs with different modes of
272 action from existing drugs. Nevertheless, several prioritized compounds were well studied
273 and had supporting evidence. A histone deacetylase (HDAC) inhibitor, vorinostat, was
274 prioritized for asthma; concordantly, HDAC inhibition was an effective treatment in an animal
275 model of asthma⁴⁶.

276 We further identified promising compounds with marginal significance (FDR < 0.1).
277 There were 123 unique compound–disease pairs with an FDR < 0.1, and mechanistic actions
278 were known for 72 compounds. The supporting literature was identified for the 26 compounds.

279 Indacaterol (a beta-2 adrenergic receptor (ADRB2) agonist) and masatinib (a proto-oncogene
280 c-Src (SRC) inhibitor) have undergone phase III clinical trials for asthma^{47,48}. There are
281 approved drugs (acetazolamide, fluorouracil, and naproxen and indomethacin, respectively)
282 with the same mechanistic action as cianidanol (a carbonic anhydrase inhibitor) and
283 raltitrexed (a thymidylate synthase inhibitor) for POAG⁴⁹, and piketoprofen and diclofenac
284 (cyclooxygenase 1/2 inhibitors) for gout, respectively. We also prioritized several compounds
285 currently under investigation, including phosphatidylinositol-3 kinase (PI3K) inhibitors for
286 asthma⁵⁰, a sodium channel inhibitor for POAG⁵¹, and a cyclooxygenase-2 (COX2) inhibitor
287 for VTE⁵². We comprehensively summarized the screened drug list and their relevant
288 evidence in **Supplementary Table 4**, which should provide genetic support to the
289 compounds under investigation and the understudied compounds. In addition, we searched
290 for structurally similar compounds (similarity > 0.85) for the compounds without known targets
291 by using BindingDB⁵³. We identified potential targets for six compounds (**Supplementary**
292 **Table 5**), which would help investigate those compounds as therapeutic candidates.

293

294

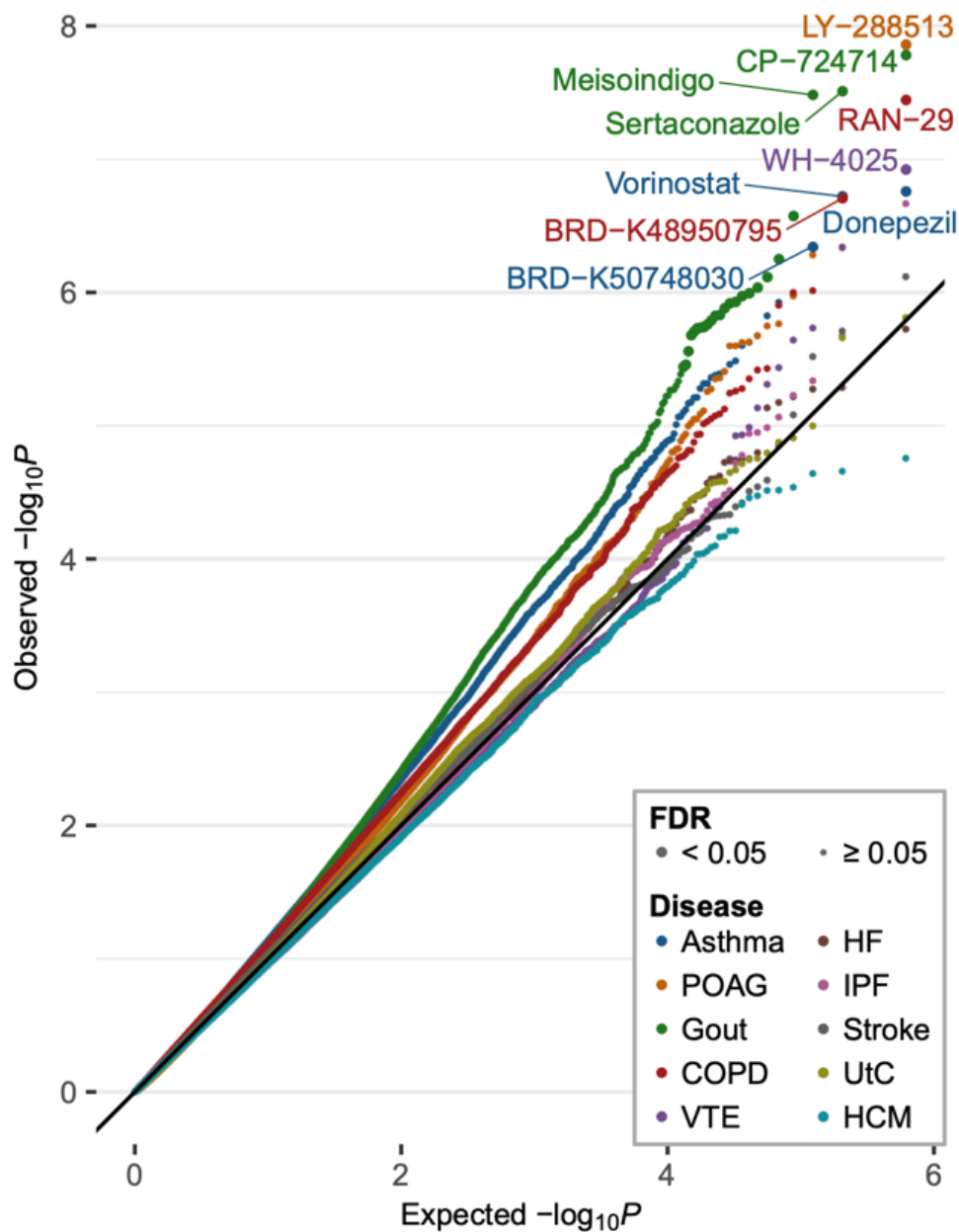


Figure 4. Negative correlation tests between genetically determined and compound-regulated gene expression profiles.

quantile–quantile plots of the negative correlation tests between genetically determined and compound-regulated gene expression profiles. Compounds with false discovery rates (FDR) <0.05 are indicated by larger dots. The compound names are shown for at most three significant compounds, for visualization purposes.

295

296

297 **Combining the three approaches for in-depth drug discovery**

298 We summarized the representative drugs and their targets, which were prioritized through
299 the three drug discovery approaches, in **Table 1**. The overlap enrichment analysis and the
300 endophenotype MR analysis identified 30 and 83 drugs for 13 and 14 drug targets,
301 respectively, and 31 compounds were nominated by the negative correlation tests. Multiple
302 components nominated drug candidates for asthma, gout, COPD, and VTE, indicating that
303 the three components were complementarily for these diseases. We noted that these
304 nominated diseases had a relatively large number of case sample sizes and genome-wide
305 significant loci. The enhanced statistical power of the GWAS for a wide range of phenotypes
306 in the framework of global biobank collaboration should contribute to the acceleration of novel
307 drug discovery. In fact, the novel loci in GBMI⁷ led to the prioritization of *PROC* for VTE (via
308 the overlap enrichment analysis) and *PLAU* for AAA (via the endophenotype MR). F11 for
309 VTE was prioritized by both the overlap enrichment analysis and endophenotype MR,
310 providing more robust evidence for F11 inhibitors from the genetic point of view. Conversely,
311 no drugs were nominated for diseases with a relatively small number of loci by either the
312 overlap enrichment analysis or negative correlation tests (e.g., IPF, UtC, and HCM). As these
313 two components require relatively large numbers of GWAS signals in their schemes, further
314 accumulation of samples is warranted.

315

Table1. Drug targets and representative drugs prioritized in this study

Disease	Overlap enrichment in disease-relevant ATC codes	Endophenotype MR	Negative correlation tests
Asthma	Ibudilast (<i>IL6</i>) Omalizumab (<i>FCER1A/FCER1G</i>)	SAR164653 (CTSA) KHK-2866 (HBEGF) Amediplase (PLAU)	Donepezil (ACHE) Vorinostat (HDAC family) BRD-K50748030 (Unknown)
POAG	-	-	LY-288513 (Unknown)
Gout	Probenecid (<i>SLC22A6/SLC22A11</i>) Lesinurad (<i>SLC22A11/SLC22A12</i>)	Anfibatide (GP1BA) Berotralstat (KLKB1)	Mesoridazine (DRD2/HTR2A) CP-724714 (Unknown) ¹
COPD	-	GMA-161 (FCGR3B)	BRD-K48950795 (Unknown) RAN-29 (Unknown)
VTE	Alteplase (<i>FGA</i>) Edoxaban (<i>F10</i>) Ancrod (<i>PROC</i>) Dabigatran etexilate (<i>F2</i>) Abelacimab (<i>F11</i>) Ecallantide (<i>KLKB1</i>) Drotrecogin alfa (<i>F5</i>)	Abelacimab (F11) CR-002 (PDGFB)	WH-4025 (Unknown)
ThC	-	Tosedostat (XPNPEP2)	(Excluded from the analysis)
AAA	-	MG-1102 (LPA) Amediplase (PLAU)	(Excluded from the analysis)
HF	-	MG-1102 (LPA)	-
IPF	-	-	-
Stroke	-	-	-
UtC	-	Anfibatide (GP1BA)	-
AcApp	-	GNF-PF-5434 (CTSB)	(Excluded from the analysis)
HCM	-	-	-

¹ Drugs without known target genes were not shown except for the drug with the lowest p-value, CP-724714. Full results can be found in **Supplementary Table 2**.

The diseases are sorted in the decreasing order of the number of the genome-wide significant loci in GBMI GWAS.

1 **Drug discovery nominated plausible candidate drugs and target genes for VTE**

2 We noted that the VTE GWAS was most successful in the screening of the drug targets: it
3 prioritized drugs corresponding to the eight drug-target genes and one compound in total
4 (**Figure 5**). All drug targets but *PDGFB* were involved in the coagulation cascade. *PDGFB*
5 has been reported to induce the expression of a tissue factor that triggers the coagulation
6 cascade⁵⁴, which underscores the strong enrichment of candidate drug targets in
7 coagulation-related genes. Of the eight drug targets, three (*PROC*, *F2*, and *F10*) were
8 targeted by the approved drugs, and two (*KLKB1* and *F11*) were targeted by drugs under
9 clinical trials for VTE, thus supporting the validity of genomics-driven drug discovery and
10 repositioning for VTE.

11

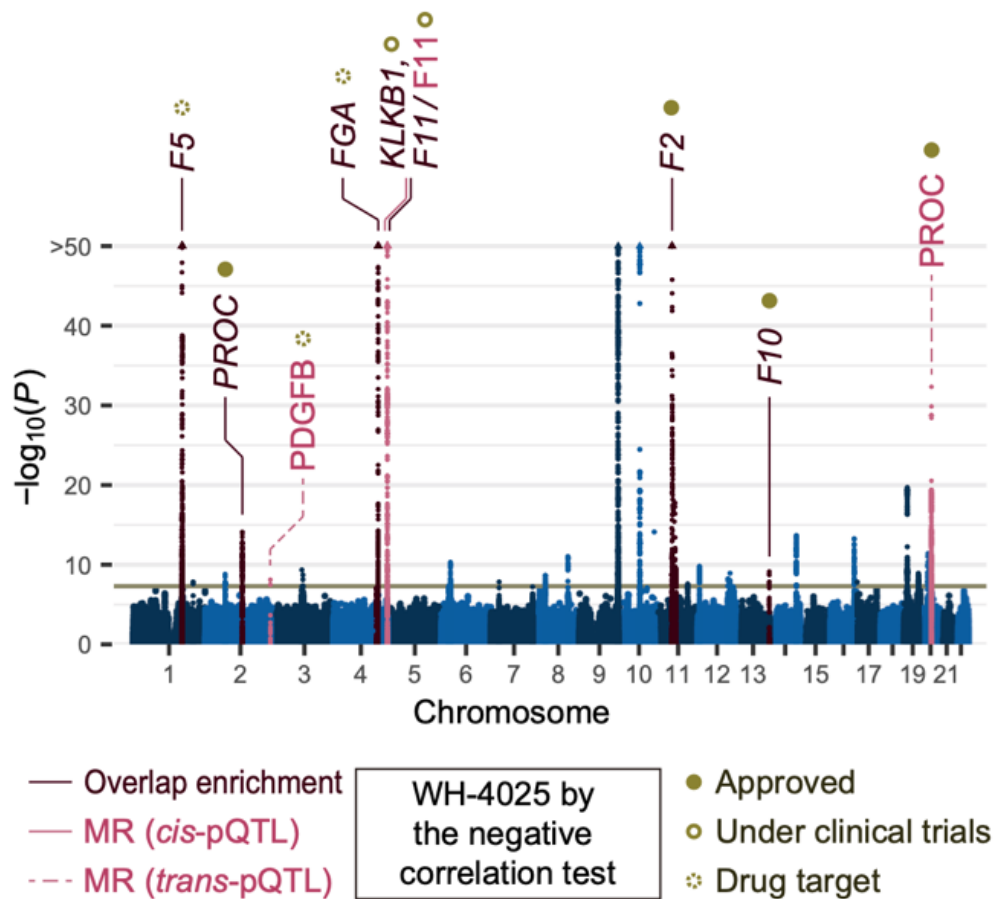


Figure 5. Drug discovery nominated plausible candidate drugs and target genes for VTE.

Drug-target genes nominated by omnibus gene prioritization and proteins nominated by Mendelian randomization (MR) are highlighted in a Manhattan plot of GBMI GWAS for VTE. The compound with a significant negative correlation between genetically regulated and compound-regulated gene expression profiles is also shown.

12

13

14 **Discussion**

15 In this study, we presented a practical framework that combined three approaches for in-
16 depth genomics-driven drug discovery, and demonstrated its utility through application to the
17 GBMI GWAS meta-analysis. Each approach has specific advantages. By focusing on the
18 genes prioritized in the disease-relevant medication codes, we obtained a list of candidate
19 drugs, most of which were indicated for the diseases. Endophenotype MR and subsequent
20 quality controls estimated the causality of proteins regarding diseases, which could not be
21 inferred by gene prioritization. Finally, the negative correlation tests of gene expression
22 profiles were able to nominate compounds with or without known target genes. Our study
23 demonstrated the importance of combining the three components for the thorough evaluation
24 of candidate drugs.

25 Multi-ethnic GWAS meta-analyses incorporated populations with diverse genetic
26 backgrounds and architectures. Matching of genetic ancestry is important to follow-up
27 functional interpretation of the GWAS results with omics information, including drug discovery.
28 To address the difference in the LD structure between populations, we used the GWAS
29 summary statistics from the population-specific meta-analysis for endophenotype MR and
30 the negative correlation tests, whereas we used those from the all-population meta-analyses
31 for gene prioritization. The differences in ancestry-matching strategies among components
32 depended on the current availability of the corresponding omics resource requested for each
33 analysis. Further accumulation of public resources with diverse ancestry should be
34 expected^{25,55}.

35 A large number of GWAS loci were required for genomics-driven drug discovery,
36 especially for the overlap enrichment analysis and the negative correlation tests. Global
37 biobank collaborations, such as GBMI, have the potential to improve the power of genetic
38 association studies to detect novel GWAS signals by incorporating diverse populations with
39 large sample sizes, and will facilitate genomics-driven drug discovery. Of note, our framework

40 successfully nominated drug candidates and their target genes, particularly for VTE, which
41 had the fifth-largest number of GWAS loci among the 13 diseases. There may be additional
42 factors other than the number of GWAS loci that are important for the success of drug
43 discovery in VTE. Among the traits with a large number of loci, VTE showed a relatively
44 modest polygenicity⁷, which might be beneficial for pinpointing the disease-relevant genes.
45 The genes implicated in the VTE GWAS were mainly centered at the coagulation cascade⁵⁶.
46 The drugs targeting coagulation factors have been under active development⁵⁷, and these
47 drugs can be promising candidates immediately repositioned to coagulation disorders other
48 than the disease for which the drugs were originally developed. The further evaluation of the
49 suitability of drug discovery for a broader range of phenotypes, including cancer, autoimmune
50 diseases, and coagulation disorders would be an interesting direction for future research.

51 There are several potential limitations for each drug discovery component. The overlap
52 enrichment analysis required the existence of the drugs approved for the disease; therefore,
53 its application to diseases without approved drugs would be challenging. Endophenotype MR
54 could be applied to proteins targeted by pQTL studies; however, the number of proteins in
55 the pQTL studies is currently limited because of the technological difficulty of proteomics⁵⁸.
56 Regarding the negative correlation tests, the LINCS L1000 compound library does not
57 contain gene expression profiles for all pairs of compounds and cell lines²¹. Therefore, we
58 used all tissue types in GTEx, regardless of disease relevance. In addition, the
59 methodological limitations of TWAS^{9,59} might affect drug discovery using GReX.

60 In conclusion, our drug discovery framework practically afforded the *in silico* screening
61 of abundant drugs and targets with supporting evidence. It enables the routine to conduct the
62 post-GWAS genomics-driven drug discovery in the era of cross-population GWAS meta-
63 analysis, which would further facilitate the translation of GWAS findings to therapeutic targets.

64

65 **Methods**

66 **GBMI GWAS meta-analysis**

67 GBMI GWAS is a meta-analysis of 18 biobanks incorporating up to 1.8 million participants
68 with diverse ancestries (341,000 EAS; 31,000 Central and South Asians; 33,000 Africans;
69 18,000 Admixed Americans; 1,600 Middle Easterners; 156,000 Finns; and 1,220,000 NFE)⁷.
70 We used the GBMI GWAS of 13 common diseases: asthma, POAG, gout, COPD, VTE, ThC,
71 AAA, HF, IPF, stroke, UtC, AcApp, and HCM. Although a GBMI GWAS was also conducted
72 for appendectomy, we excluded this trait because it was a procedure endpoint rather than a
73 disease.

74

75 **Gene prioritization**

76 We used four tools for gene prioritization from GWAS summary statistics, i.e., MAGMA,
77 DEPICT, Pi, and PoPS. We used the default settings, unless otherwise stated. Variants with
78 P -values $< 1.0 \times 10^{-5}$ were used as input for DEPICT. We followed the original paper for the
79 setup of Pi⁵. Specifically, we used the lead variants with $P < 5.0 \times 10^{-8}$ as input, eQTL in the
80 peripheral blood and immune cells, chromatin interaction in immune cells, topologically
81 associating domain boundary in the GM12878 cell line, and the STRING⁶¹ protein–protein
82 interaction network, with a high confidence score. PoPS was originally developed to pinpoint
83 one responsible gene per locus, and chooses the gene with the highest score at the locus of
84 interest²⁴. Here, we used top-ranked genes, rather than pinpointed genes, to incorporate
85 multiple genes per locus for drug discovery. We used the summary statistics of the all-
86 population GWAS meta-analyses as input and the European subset of the 1000 Genomes
87 Project (Phase 3) as a reference, given that more than half of the GBMI samples were NFE⁷.
88 We prioritized genes with conventional thresholds, i.e., FDR < 0.05 for MAGMA, and top 5%
89 of the genes in the descending order of gene scores for Pi and PoPS. We used an FDR $<$
90 0.2 for DEPICT, as DEPICT calculates P -values only for the genes in the pre-featured target

91 loci, by default. When we examined sequentially changed thresholds as a sensitivity analysis,
92 we used FDR thresholds of 0.001, 0.005, 0.01, 0.05, 0.1, 0.2, and 0.5 for MAGMA and
93 DEPICT. Pi and PoPS calculate the gene score instead of FDR. We used the top 1%, 5%,
94 and 10% of the genes with the highest gene scores. In addition, a Pi score > 1.5, 2.0, 2.5,
95 and 3.0 for Pi, and a PoPS score > 0, 0.5, 1.0, 1.5, and 2 for PoPS were also examined.

96

97 **Enrichment analysis of drug indication categories**

98 We used the list of prioritized genes as input to perform a series of Fisher's exact tests for
99 ATC or ICD-10 codes, to test the enrichment of drug-target genes in particular codes. We
100 used the drug-target database provided by GREP¹⁴, which was constructed by curating two
101 major drug databases, Drug Bank and TTD. The ICD-10 codes were summarized into the 21
102 large categories, as shown in **Supplementary Figure 2**. Because ICD-10 is a disease-
103 classification system, we simply defined the relevant ICD-10 category as the category that
104 contained the disease. Conversely, ATC is a drug-classification system, and the approved
105 drugs can belong to multiple ATC codes. Therefore, we defined the disease-relevant ATC
106 code as the ATC code with the largest number of approved drugs for the disease-relevant
107 ICD-10 category. We defined the disease-irrelevant ATC codes as the ATC codes without any
108 approved drugs for the disease-relevant ICD-10 category. Regarding ATC, we limited the
109 enrichment analyses to the diseases for which there were more than four approved drugs in
110 the disease-relevant ATC codes. As a result, four diseases (i.e., AAA, IPF, AcApp, and HCM)
111 were excluded.

112

113 **Mendelian randomization of the pQTL signals**

114 We used Wald ratio tests for MR analyses. The lead variants of the five protein QTL studies^{27–}
115 ³¹ were evaluated as described previously¹⁸. We used the lead variants of drug-target
116 proteins classified as tier 1 variants as instrumental variables. The tier 1 variants were defined

117 as the variants that were associated with no more than five proteins and did not show
118 heterogeneity in the five studies. When the lead variant of the pQTL was missing in the GBMI
119 GWAS summary statistics, we used a proxy variant with the largest R^2 , if the R^2 was larger
120 than 0.8. We checked the directionality of causal relationships using Steiger filtering⁶². MR
121 analyzes were performed using the “TwoSampleMR” R package⁶³.

122

123 **Colocalization analysis**

124 To test colocalization in the presence of multiple causal variants, we applied coloc to the
125 signals decomposed by SuSiE³² for each locus, including the variants located within ± 500
126 kb of the lead variant (coloc + SuSiE). If SuSiE³⁴ did not converge in 100 iterations for either
127 pQTL or GBMI GWAS, we instead used coloc³³. Coloc + SuSiE and coloc were performed
128 using their default parameters. The summary statistics were not publicly available for two
129 pQTL studies^{30,31}; therefore, we compared R^2 between the lead variants of the pQTL and the
130 GBMI GWAS for those studies. We considered that the signals of pQTL and GBMI GWAS
131 were colocalized if the maximum posterior probability of colocalization (i.e., PP.H4 for coloc
132 and coloc + SuSiE) was larger than 0.8, or the R^2 between the lead variants was larger than
133 0.8.

134

135 **Negative correlation tests between genetically determined and compound-regulated** 136 **gene expression**

137 We utilized Trans-Phar¹⁶ for the negative correlation tests. Trans-Phar internally used
138 FOCUS⁶⁴ to infer disease case–control GReX for 44 GTEx v7 tissues based on the GWAS
139 summary statistics. Compound-regulated gene expression profiles were obtained from the
140 LINCS L1000 library. We calculated Spearman’s rho between GReX and compound-
141 regulated gene expression profiles using the GReX inferred from the NFE-specific and EAS-

142 specific GWAS meta-analyses, separately. The correlation coefficients were combined by a
143 random-effect model using the R package “metacor.”

144

145 **Filtering GWAS summary statistics based on effective sample sizes**

146 Because of the diverse ancestry in the GWASs for meta-analysis, there was remarkable
147 heterogeneity in the effective sample sizes across the genome-wide variants of the GBMI
148 results of each phenotype. This heterogeneity affected the performance of downstream
149 analyses, including those of polygenic risk score⁶⁵. Therefore, we excluded variants with
150 effective sample sizes <50% of the maximum effective sample size from the GWAS summary
151 statistics of each phenotype.

152

153 **Data and code availability**

154 The GBMI GWAS summary statistics are publicly available at
155 <https://www.globalbiobankmeta.org/resources>. The genomics-driven drug discovery analysis
156 was conducted using the following publicly available tools: MAGMA
157 (<https://ctg.cncr.nl/software/magma>), DEPICT (<https://data.broadinstitute.org/mpg/depict/>),
158 PoPS (<https://github.com/FinucaneLab/pops>), GREP
159 (<https://github.com/saorisakaue/GREP>), Trans-Phar (<https://github.com/konumat/Trans-Phar>), LocusZoom (<http://locuszoom.org/>), and the Pi, TwoSampleMR, coloc, susieR, and
160 metacor R packages.
161

162

163 **Author contributions**

164 S.N., T.K. and Y.O. designed the study, and wrote the manuscript. S.N., T.K., K.H.W., and
165 W.Z. conducted data analysis. Y.O. supervised the study.

166

167 **Declare of interests**

168 The authors declare no competing interests.

169

170 References

- 171 1. Hay, M., Thomas, D. W., Craighead, J. L., Economides, C. & Rosenthal, J. Clinical
172 development success rates for investigational drugs. *Nat. Biotechnol.* **32**, 40–51
173 (2014).
- 174 2. Nelson, M. R. *et al.* The support of human genetic evidence for approved drug
175 indications. *Nat. Genet.* **47**, 856–860 (2015).
- 176 3. King, E. A., Davis, J. W. & Degner, J. F. Are drug targets with genetic support twice
177 as likely to be approved? Revised estimates of the impact of genetic support for drug
178 mechanisms on the probability of drug approval. *PLoS Genet.* **15**, e1008489 (2019).
- 179 4. Sabatine, M. S. *et al.* Evolocumab and Clinical Outcomes in Patients with
180 Cardiovascular Disease. *N. Engl. J. Med.* **376**, 1713–1722 (2017).
- 181 5. Fang, H. *et al.* A genetics-led approach defines the drug target landscape of 30
182 immune-related traits. *Nat. Genet.* **51**, 1082–1091 (2019).
- 183 6. Reay, W. R. & Cairns, M. J. Advancing the use of genome-wide association studies
184 for drug repurposing. *Nat. Rev. Genet.* **22**, 658–671 (2021).
- 185 7. Zhou, W. *et al.* Global Biobank Meta-analysis Initiative: power genetic discovery for
186 human diseases with > 2.6 million samples across diverse ancestries. *medRxiv*
187 (2021) doi:10.1101/2021.11.19.21266436.
- 188 8. Sakaue, S. *et al.* A cross-population atlas of genetic associations for 220 human
189 phenotypes. *Nat. Genet.* **53**, 1415–1424 (2021).
- 190 9. Wainberg, M. *et al.* Opportunities and challenges for transcriptome-wide association
191 studies. *Nat. Genet.* **51**, 592–599 (2019).
- 192 10. Kuchenbaecker, K. *et al.* The transferability of lipid loci across African, Asian and
193 European cohorts. *Nat. Commun.* **10**, 4330 (2019).
- 194 11. Shi, H. *et al.* Population-specific causal disease effect sizes in functionally important
195 regions impacted by selection. *Nat. Commun.* **12**, 1098 (2021).
- 196 12. Okada, Y. *et al.* Genetics of rheumatoid arthritis contributes to biology and drug
197 discovery. *Nature* **506**, 376–381 (2013).
- 198 13. Malik, R. *et al.* Multiancestry genome-wide association study of 520,000 subjects
199 identifies 32 loci associated with stroke and stroke subtypes. *Nat. Genet.* **50**, 524–
200 537 (2018).
- 201 14. Sakaue, S. & Okada, Y. GREP: Genome for REPositioning drugs. *Bioinformatics* **35**,
202 3821–3823 (2019).
- 203 15. Zhou, S. *et al.* A Neanderthal OAS1 isoform Protects Against COVID-19
204 Susceptibility and Severity: Results from Mendelian Randomization and Case-Control
205 Studies. *medRxiv* (2020) doi:10.1101/2020.10.13.20212092.
- 206 16. Konuma, T., Ogawa, K. & Okada, Y. Integration of genetically regulated gene
207 expression and pharmacological library provides therapeutic drug candidates. *Hum.*

- 208 *Mol. Genet.* **30**, 294–304 (2021).
- 209 17. Sonehara, K. & Okada, Y. Genomics-driven drug discovery based on disease-
210 susceptibility genes. doi:10.1186/s41232-021-00158-7.
- 211 18. Zheng, J. *et al.* Phenome-wide Mendelian randomization mapping the influence of the
212 plasma proteome on complex diseases. *Nat. Genet.* **52**, 1122–1131 (2020).
- 213 19. So, H.-C. *et al.* Analysis of genome-wide association data highlights candidates for
214 drug repositioning in psychiatry. *Nat. Neurosci.* **20**, 1342–1349 (2017).
- 215 20. Aguet, F. *et al.* Genetic effects on gene expression across human tissues. *Nature*
216 **550**, 204–213 (2017).
- 217 21. Subramanian, A. *et al.* A Next Generation Connectivity Map: L1000 Platform and the
218 First 1,000,000 Profiles. *Cell* **171**, 1437-1452.e17 (2017).
- 219 22. Leeuw, C. A. de, Mooij, J. M., Heskes, T. & Posthuma, D. MAGMA: Generalized
220 Gene-Set Analysis of GWAS Data. *PLOS Comput. Biol.* **11**, e1004219 (2015).
- 221 23. Pers, T. H. *et al.* Biological interpretation of genome-wide association studies using
222 predicted gene functions. *Nat. Commun.* **6**, 5890 (2015).
- 223 24. Weeks, E. M. *et al.* Leveraging polygenic enrichments of gene features to predict
224 genes underlying complex traits and diseases. *medRxiv* **23**, (2020).
- 225 25. Zhao, H. *et al.* Proteome-wide Mendelian randomization in global biobank meta-
226 analysis reveals trans-ancestry drug targets for common diseases. *medRxiv* (2021).
- 227 26. Vösa, U. *et al.* Large-scale cis- and trans-eQTL analyses identify thousands of
228 genetic loci and polygenic scores that regulate blood gene expression. *Nat. Genet.*
229 *2021 539* **53**, 1300–1310 (2021).
- 230 27. Sun, B. B. *et al.* Genomic atlas of the human plasma proteome. *Nature* **558**, 73–79
231 (2018).
- 232 28. Suhre, K. *et al.* Connecting genetic risk to disease end points through the human
233 blood plasma proteome. *Nat. Commun.* **8**, 14357 (2017).
- 234 29. Folkersen, L. *et al.* Mapping of 79 loci for 83 plasma protein biomarkers in
235 cardiovascular disease. *PLOS Genet.* **13**, e1006706 (2017).
- 236 30. Emilsson, V. *et al.* Co-regulatory networks of human serum proteins link genetics to
237 disease. *Science (80-.)*. **361**, 769–773 (2018).
- 238 31. Yao, C. *et al.* Genome-wide mapping of plasma protein QTLs identifies putatively
239 causal genes and pathways for cardiovascular disease. *Nat. Commun.* **9**, 3268
240 (2018).
- 241 32. Wallace, C. A more accurate method for colocalisation analysis allowing for multiple
242 causal variants. *PLOS Genet.* **17**, e1009440 (2021).
- 243 33. Giambartolomei, C. *et al.* Bayesian Test for Colocalisation between Pairs of Genetic
244 Association Studies Using Summary Statistics. *PLOS Genet.* **10**, e1004383 (2014).
- 245 34. Wang, G., Sarkar, A., Carbonetto, P. & Stephens, M. A simple new approach to

- 246 variable selection in regression, with application to genetic fine mapping. *J. R. Stat.*
247 *Soc. Ser. B (Statistical Methodol.* **82**, 1273–1300 (2020).
- 248 35. Kotani, K. *et al.* Lipoprotein(a) Levels in Patients With Abdominal Aortic Aneurysm.
249 *Angiology* **68**, 99–108 (2017).
- 250 36. Bruzelius, M. *et al.* PDGFB, a new candidate plasma biomarker for venous
251 thromboembolism: results from the VEREMA affinity proteomics study. *Blood* **128**,
252 e59–e66 (2016).
- 253 37. Liu, J. *et al.* Associations of ApoA1 and ApoB–Containing Lipoproteins With AngII–
254 Induced Abdominal Aortic Aneurysms in Mice. *Arterioscler. Thromb. Vasc. Biol.* **35**,
255 1826–1834 (2015).
- 256 38. Wishart, D. S. *et al.* DrugBank 5.0: a major update to the DrugBank database for
257 2018. *Nucleic Acids Res.* **46**, D1074–D1082 (2018).
- 258 39. Chen, X., Ji, Z. L. & Chen, Y. Z. TTD: Therapeutic Target Database. *Nucleic Acids*
259 *Res.* **30**, 412–415 (2002).
- 260 40. Whirl-Carrillo, M. *et al.* An Evidence-Based Framework for Evaluating
261 Pharmacogenomics Knowledge for Personalized Medicine. *Clin. Pharmacol. Ther.*
262 **110**, 563–572 (2021).
- 263 41. Ochoa, D. *et al.* Open Targets Platform: supporting systematic drug–target
264 identification and prioritisation. *Nucleic Acids Res.* **49**, D1302–D1310 (2021).
- 265 42. Sala, V. *et al.* Cardiac concentric hypertrophy promoted by activated Met receptor is
266 mitigated in vivo by inhibition of Erk1,2 signalling with Pimasertib. *J. Mol. Cell.*
267 *Cardiol.* **93**, 84–97 (2016).
- 268 43. A, M., W, W., F, S., S, H. & HJ, W. Mitogen-activated protein kinase kinase 1/2
269 inhibition and angiotensin II converting inhibition in mice with cardiomyopathy caused
270 by lamin A/C gene mutation. *Biochem. Biophys. Res. Commun.* **452**, 958–961 (2014).
- 271 44. Verhamme, P. *et al.* Abrelcimab for Prevention of Venous Thromboembolism. *N.*
272 *Engl. J. Med.* **385**, 609–617 (2021).
- 273 45. Kuramoto, E. *et al.* Inhalation of urokinase-type plasminogen activator reduces airway
274 remodeling in a murine asthma model. *Am. J. Physiol. Cell. Mol. Physiol.* **296**, L337–
275 L346 (2009).
- 276 46. Ren, Y. *et al.* Therapeutic effects of histone deacetylase inhibitors in a murine asthma
277 model. *Inflamm. Res.* **65**, 995–1008 (2016).
- 278 47. van Zyl-Smit, R. N. *et al.* Once-daily mometasone plus indacaterol versus
279 mometasone or twice-daily fluticasone plus salmeterol in patients with inadequately
280 controlled asthma (PALLADIUM): a randomised, double-blind, triple-dummy,
281 controlled phase 3 study. *Lancet Respir. Med.* **8**, 987–999 (2020).
- 282 48. Chanez, P. *et al.* Masitinib Significantly Decreases the Rate of Asthma Exacerbations
283 in Patients with Severe Asthma Uncontrolled by Oral Corticosteroids: A Phase 3

- 284 Multicenter Study. in *B93. LATE BREAKING CLINICAL TRIALS IN AIRWAY*
285 *DISEASES* A4210–A4210 (American Thoracic Society, 2020). doi:10.1164/ajrccm-
286 conference.2020.201.1_MeetingAbstracts.A4210.
- 287 49. Lo Faro, V. *et al.* Global Biobank Meta-Analysis Initiative: A genome-wide association
288 meta-analysis identifies novel primary open-angle glaucoma loci and shared biology
289 with vascular and cell proliferation mechanisms. *medRxiv* (2021).
- 290 50. Yoo, E. J., Ojiaku, C. A., Sunder, K. & Panettieri, R. A. Phosphoinositide 3-Kinase in
291 Asthma: Novel Roles and Therapeutic Approaches. *Am. J. Respir. Cell Mol. Biol.* **56**,
292 700–707 (2017).
- 293 51. Hains, B. C. & Waxman, S. G. Neuroprotection by Sodium Channel Blockade with
294 Phenytoin in an Experimental Model of Glaucoma. *Investig. Ophthalmology Vis. Sci.*
295 **46**, 4164 (2005).
- 296 52. Anderson, D. R. *et al.* Aspirin or Rivaroxaban for VTE Prophylaxis after Hip or Knee
297 Arthroplasty. *N. Engl. J. Med.* **378**, 699–707 (2018).
- 298 53. Gilson, M. K. *et al.* BindingDB in 2015: A public database for medicinal chemistry,
299 computational chemistry and systems pharmacology. *Nucleic Acids Res.* **44**, D1045–
300 D1053 (2016).
- 301 54. Gebhard, C. *et al.* PDGF-CC induces tissue factor expression: role of PDGF receptor
302 α/β . *Basic Res. Cardiol.* **105**, 349–356 (2010).
- 303 55. Martin, A. R. *et al.* Clinical use of current polygenic risk scores may exacerbate health
304 disparities. *Nat. Genet.* **51**, 584–591 (2019).
- 305 56. Wolford, B. N. *et al.* Multi-ancestry GWAS for venous thromboembolism identifies
306 novel loci followed by experimental validation. *medRxiv* (2021).
- 307 57. Grover, S. P. & Mackman, N. Intrinsic Pathway of Coagulation and Thrombosis.
308 *Arterioscler. Thromb. Vasc. Biol.* **39**, 331–338 (2019).
- 309 58. Pietzner, M. *et al.* Mapping the proteo-genomic convergence of human diseases.
310 *Science (80-.)*. **374**, eabj1541 (2021).
- 311 59. Leeuw, C. de, Werme, J., Savage, J., Peyrot, W. & Posthuma, D. Reconsidering the
312 validity of transcriptome-wide association studies. *bioRxiv* (2021)
313 doi:10.1101/2021.08.15.456414.
- 314 60. Pruim, R. J. *et al.* LocusZoom: regional visualization of genome-wide association
315 scan results. *Bioinformatics* **26**, 2336 (2010).
- 316 61. Szklarczyk, D. *et al.* The STRING database in 2011: functional interaction networks of
317 proteins, globally integrated and scored. *Nucleic Acids Res.* **39**, (2011).
- 318 62. Hemani, G., Tilling, K. & Smith, G. D. Orienting the causal relationship between
319 imprecisely measured traits using GWAS summary data. *PLOS Genet.* **13**, e1007081
320 (2017).
- 321 63. Hemani, G. *et al.* The MR-base platform supports systematic causal inference across

- 322 the human phenome. *Elife* **7**, 1–29 (2018).
- 323 64. Mancuso, N. *et al.* Probabilistic fine-mapping of transcriptome-wide association
324 studies. *Nat. Genet.* **51**, 675–682 (2019).
- 325 65. Wang, Y. *et al.* Global biobank analyses provide lessons for computing polygenic risk
326 scores across diverse cohorts. *medRxiv* (2021) doi:10.1101/2021.11.18.21266545.
- 327
- 328